Rapid #: -10665858

CROSS REF ID: **1023734**

LENDER: **GZM :: EJournals**

BORROWER: **LDL :: Main Library**

TYPE:	Article CC:CCL
JOURNAL TITLE:	Nuclear instruments & methods in physics research. Section A, Accelerators, spectrometers, detectors and associated equipment
USER JOURNAL TITLE:	NUCLEAR INSTRUMENTS & METHODS IN PHYSICS RESEARCH SECTION A-ACCELERATORS SPECTROMETERS DETECTORS AND ASSOCIATED EQUIPMENT
ARTICLE TITLE:	FARADAY-ROTATION OF OPTICALLY PUMPED SODIUM VAPOR IN A WEAK MAGNETIC-FIELD
ARTICLE AUTHOR:	UENO, A
VOLUME:	262
ISSUE:	2-3
MONTH:	
YEAR:	1987
PAGES:	170-178
ISSN:	0168-9002
OCLC #:	

Processed by RapidX: 5/31/2016 9:28:53 AM

Nuclear Instruments and Methods in Physics Research A262 (1987) 170–178
North-Holland, Amsterdam

FARADAY ROTATION OF OPTICALLY PUMPED SODIUM VAPOUR IN A WEAK MAGNETIC FIELD

Akira UENO, Kouji TAKASAKI, Kouichi OGURA, Yoshihisa WAKUTA and Isao KUMABE
Faculty of Engineering, Kyushu University, Fukuoka, 812, Japan

Kiyoshi O-OHATA
College of General Education, Kyushu University, Fukuoka, 812, Japan

Yoshiharu MORI and Sadayoshi FUKUMOTO
National Laboratory for High Energy Physics, Oho-machi, Tsukuba-gun, Ibaraki-ken, 305, Japan

Received 21 May 1987

Faraday rotation of optically pumped sodium atoms in a weak magnetic field, which is lower than the critical field of hyperfine splitting, was obtained theoretically. The estimated rotation angles were compared with the experiments for various magnetic fields. The measured values showed good agreement with the values calculated from the theory.

1. Introduction

Recently, optical pumping with intense lasers has been applied to generate nuclear-spin polarized hydrogen atoms. Since there is no laser having the frequency which is matched to an appropriate resonance of the hydrogen atom, indirect methods to pump the hydrogen atom, such as the reactions of spin-charge exchange or spin exchange between hydrogen atoms and other optically pumped atoms have been currently used. The method which was proposed by Anderson was based on the spin-charge exchange reactions between protons and optically oriented sodium atoms [1]. At KEK, this idea has been realized as the intense polarized H^- ion source for the 12 GeV proton synchrotron [2]. Happer et al. have shown that in a mixture of xenon and rubidium, the nuclear spin of xenon atoms are largely polarized by spin-exchange reactions with optically pumped rubidium atoms [3]. This procedure could be applied to produce a sufficiently thick polarized hydrogen gas which would be very attractive for nuclear fusion with polarized atoms [4]. Recently, a new idea called collisional pumping, which is based on the multistage charge-exchange reactions between hydrogen atoms and polarized sodium atoms in a low magnetic field has been proposed by Anderson et al. [5].

In these applications, it is crucial to measure the atomic polarization of optically pumped atoms accurately because the nuclear polarization is directly related to the atomic polarization. A very useful method, which is based on Faraday rotation (paramagnetic rotation) in optically oriented atoms, has been employed so far to measure the atomic polarization [6]. This scheme, however, has been only applied to analyze the atomic polarization in a strong magnetic field, where the nuclear-spin state does not couple with the atomic-spin state and the contributions from the many hyperfine sublevels can be neglected, so that the theoretical treatment becomes very simple.

On the other hand, optical pumping in a weak magnetic field is essential in some applications such as collisional pumping. A nuclear-spin polarization is made by the hyperfine interactions between sublevels in a weak magnetic field lower than the critical field strength. Therefore, it is worthwhile estimating the Faraday rotation in a weak magnetic field.

The treatment for the Faraday rotation in this report can be applied for any strength of the magnetic field. The results of calculations were compared with experiment.

2. Faraday rotation in weak magnetic field

For hydrogenlike atoms, the external magnetic field can be specified by the critical magnetic field B_c defined by the following equation:

$$B_c = \frac{\Delta W}{\beta_e(g_I + g_e)}. \tag{1}$$

0168-9002/87/$03.50

Here, ΔW is the hyperfine energy, β_e is Bohr magneton, g_I and g_e are the g-factors of nucleus and electron, respectively. For the case of sodium atoms, B_c is 632 G.

In a strong magnetic field larger than B_c, the effect of the coupling between J and nuclear spin I can be neglected. Here, J is the sum of the electronic orbital angular momentum L and spin S. Each Zeeman sublevel is specified by m_J and m_I which are the Z-components of J and I, respectively.

On the other hand, when the magnetic field is lower than the critical field, J and I cannot be decoupled and $F = I + J$ becomes a good quantum number. In this case, Zeeman sublevels are specified by m_F. The energy diagram of the Zeeman sublevels of sodium ground states (3S) and excited states (3P) is shown, schematically, in fig. 1. The wave functions of each ground and excited sublevel can be written as follows:
ground state:

$$\phi_i = |m_L\rangle\left(A_i|m_S=1/2\rangle|m_I\rangle + B_i|m_S=-1/2\rangle|m_I\rangle\right) \quad (i=1\to 8); \tag{2a}$$

excited state:

$$\phi'_j = \left(A'_j|m_L\rangle|m_S=1/2\rangle + B'_j|m_L\rangle|m_S=-1/2\rangle\right)|m_I\rangle \quad (j=1\to 6). \tag{2b}$$

All of the wave functions of sublevels for each state are summarized in table 1.

The coefficients A_i, B_i, A'_j and B'_j are varied as a function of the external magnetic field strength. The calculated values are summarized in table 2. A parameter χ, which represents the strength of the magnetic field B, is defined by the following equation:

$$\chi = \frac{B}{B_c}. \tag{3}$$

The Faraday rotation angle can be calculated by the following equation:

$$\theta = \frac{\pi l \nu}{c}(n_+ - n_-). \tag{4}$$

Here, n_+ and n_- are the refractive indices for left and right circular polarized light, ν is the frequency of the light and l is the length of the target. The refractive index n is given by the following equation with $x_{ij} = \pi\tau(\nu_{ij} - \nu)$ as shown in ref. [6],

$$n - 1 = \frac{q_{3P}c^2 N}{8\pi^2}\sum_i\sum_j \frac{x_{ij}}{1+x_{ij}^2}P_i\beta_{ij}, \tag{5}$$

where i and j specify the sublevels of the ground state and the excited state, q_{3P} is the statistical weight of the excited states, ν_{ij} is the frequency of the transition between the ith state and the jth state, N is the density of sodium atoms, τ is the lifetime of 3P states, P_i is the occupation probability of the ith state, and β_{ij} is the

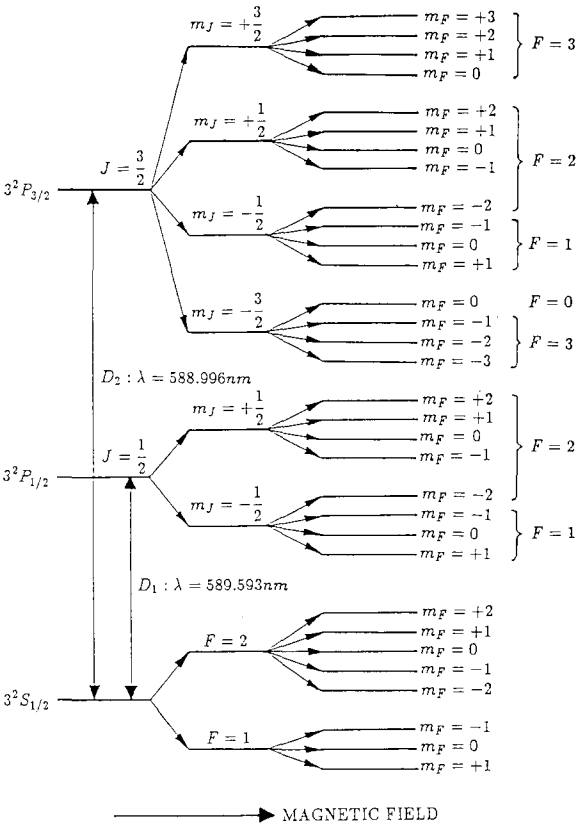

Fig. 1. Energy diagram of the Zeeman sublevels of the sodium ground state (3S) and excited state (3P).

relative strength of the transition between the ith state and the jth state. If we consider D_1 and D_2 to be resonant lines, the rotation angle θ can be derived from eqs. (4) and (5),

$$\theta = \frac{q_{3P}c^2\nu Nl}{8\pi}\left\{\sum_i\sum_j \psi_{ij}P_i\beta_{ij}^+ - \sum_i\sum_j \psi_{ij}P_i\beta_{ij}^-\right\}, \tag{6}$$

where

$$\psi_{ij} = \frac{x_{ij}}{\nu_{ij}^3\left(1+x_{ij}^2\right)}.$$

Here β_{ij}^+ and β_{ij}^-, which can be derived from the coefficients A_i, B_i, A'_j and B'_j, are the transition probabilities induced by left and right circular polarized light respectively, and those are summarized in table 3.

We define θ_0 and θ_P by following equations

$$\theta = \theta_0 + \theta_P, \tag{7}$$

$$\theta_0 = \frac{q_{3P}c^2\nu Nl}{8\pi}\left\{\sum_i\sum_j \frac{\psi_{ij}\beta_{ij}^+}{8} - \sum_i\sum_j \frac{\psi_{ij}\beta_{ij}^-}{8}\right\}, \tag{8}$$

Table 1
Hyperfine sublevels of the sodium ground state (3S) and excited state (3P).
(a) 3P states

j	J	m_J	Wave function	$(F \quad m_F)$
1	3/2	3/2	$A_1'\|1\rangle\|1/2\rangle\begin{cases}\|3/2\rangle\\ \|1/2\rangle\\ \|-1/2\rangle\\ \|-3/2\rangle\end{cases}$	(3 3) (3 2) (3 1) (3 0)
2	3/2	1/2	$(A_2'\|0\rangle\|1/2\rangle + B_2'\|1\rangle\|-1/2\rangle)\begin{cases}\|3/2\rangle\\ \|1/2\rangle\\ \|-1/2\rangle\\ \|-3/2\rangle\end{cases}$	(2 2) (2 1) (2 0) (2 −1)
3	3/2	−1/2	$(A_3'\|-1\rangle\|1/2\rangle + B_3'\|0\rangle\|-1/2\rangle)\begin{cases}\|3/2\rangle\\ \|1/2\rangle\\ \|-1/2\rangle\\ \|-3/2\rangle\end{cases}$	(2 −2) (1 −1) (1 0) (1 1)
4	3/2	−3/2	$B_4'\|-1\rangle\|-1/2\rangle\begin{cases}\|3/2\rangle\\ \|1/2\rangle\\ \|-1/2\rangle\\ \|-3/2\rangle\end{cases}$	(0 0) (3 −1) (3 −2) (3 −3)
5	1/2	1/2	$(A_5'\|0\rangle\|1/2\rangle + B_5'\|1\rangle\|-1/2\rangle)\begin{cases}\|3/2\rangle\\ \|1/2\rangle\\ \|-1/2\rangle\\ \|-3/2\rangle\end{cases}$	(2 2) (2 1) (2 0) (2 −1)
6	1/2	−1/2	$(A_6'\|-1\rangle\|1/2\rangle + B_6'\|0\rangle\|-1/2\rangle)\begin{cases}\|3/2\rangle\\ \|1/2\rangle\\ \|-1/2\rangle\\ \|-3/2\rangle\end{cases}$	(2 −2) (1 −1) (1 0) (1 1)

(b) 3S states

i	F	m_F	Wave function
1	2	2	$\|0\rangle(A_1\|1/2\rangle\|3/2\rangle)$
2	2	1	$\|0\rangle(A_2\|1/2\rangle\|1/2\rangle + B_2\|-1/2\rangle\|3/2\rangle)$
3	2	0	$\|0\rangle(A_3\|1/2\rangle\|-1/2\rangle + B_3\|-1/2\rangle\|1/2\rangle)$
4	2	−1	$\|0\rangle(A_4\|1/2\rangle\|-3/2\rangle + B_4\|-1/2\rangle\|-1/2\rangle)$
5	2	−2	$\|0\rangle(B_5\|-1/2\rangle\|-3/2\rangle)$
6	1	−1	$\|0\rangle(A_6\|1/2\rangle\|-3/2\rangle + B_6\|-1/2\rangle\|-1/2\rangle)$
7	1	0	$\|0\rangle(A_7\|1/2\rangle\|-1/2\rangle + B_7\|-1/2\rangle\|1/2\rangle)$
8	1	1	$\|0\rangle(A_8\|1/2\rangle\|1/2\rangle + B_8\|-1/2\rangle\|3/2\rangle)$

$$\theta_P = \frac{q_{3P} c^2 \nu N l}{8\pi}\left\{\sum_i \sum_j \psi_{ij}\beta_{ij}^{+}\left(P_i - \tfrac{1}{8}\right) - \sum_i \sum_j \psi_{ij}\beta_{ij}^{-}\left(P_i - \tfrac{1}{8}\right)\right\}. \tag{9}$$

Here, θ_0 is the rotation angle when the sodium target is unpolarized ($P_i = \frac{1}{8}$) and θ_P is the additional Faraday rotation produced by the polarized sodium vapour.

The target thickness Nl can be estimated from eq. (7) by measuring the Faraday rotation angle of θ_0.

Zeeman splittings of the ground state atoms can be neglected at the low magnetic field compared with the energy difference between $3P_{1/2}$ and $3P_{3/2}$. Therefore, ψ_{ij} for each $3P_{1/2}$ and $3P_{3/2}$ states can be shown as the following equations

$$\psi_{ij}(3P_{1/2}) \simeq \psi_{1/2} = \frac{x_{1/2}}{\nu_{1/2}^3\left(1 + x_{1/2}^2\right)}, \tag{10a}$$

$$\psi_{ij}(3P_{3/2}) \simeq \psi_{3/2} = \frac{x_{3/2}}{\nu_{3/2}^3\left(1 + x_{3/2}^2\right)}, \tag{10b}$$

where, $\nu_{1/2}$ and $\nu_{3/2}$ are the frequencies of D_1 and D_2

Table 2
Clebsch–Gordan coefficients of each hyperfine sublevels of the sodium ground state (3S) and excited state (3P).
(a) 3P states

j	A'_j	B'_j
1	1	0
2	$\sqrt{2/3}$	$\sqrt{1/3}$
3	$\sqrt{1/3}$	$\sqrt{2/3}$
4	0	1
5	$-\sqrt{1/3}$	$\sqrt{2/3}$
6	$-\sqrt{2/3}$	$\sqrt{1/3}$

(b) 3S states

i	A_i	B_i
1	1	0
2	$\frac{\sqrt{3}}{2}\frac{1}{\sqrt{2(1+x+x^2)-(1+2x)\sqrt{1+x+x^2}}}$	$\frac{1}{2}\frac{-(1+2x)+2\sqrt{1+x+x^2}}{\sqrt{2(1+x+x^2)-(1+2x)\sqrt{1+x+x^2}}}$
3	$\frac{1}{\sqrt{2}}\frac{1}{\sqrt{(1+x^2)-x\sqrt{1+x^2}}}$	$\frac{1}{\sqrt{2}}\frac{-x+\sqrt{1+x^2}}{\sqrt{(1+x^2)-x\sqrt{1+x^2}}}$
4	$\frac{\sqrt{3}}{2}\frac{1}{\sqrt{2(1-x+x^2)+(1-2x)\sqrt{1-x+x^2}}}$	$\frac{1}{2}\frac{(1-2x)+2\sqrt{1-x+x^2}}{\sqrt{2(1-x+x^2)+(1-2x)\sqrt{1-x+x^2}}}$
5	0	1
6	$\frac{\sqrt{3}}{2}\frac{1}{\sqrt{2(1-x+x^2)-(1-2x)\sqrt{1-x+x^2}}}$	$\frac{1}{2}\frac{(1-2x)-2\sqrt{1-x+x^2}}{\sqrt{2(1-x+x^2)-(1-2x)\sqrt{1-x+x^2}}}$
7	$\frac{1}{\sqrt{2}}\frac{1}{\sqrt{2(1+x^2)+x\sqrt{1+x^2}}}$	$\frac{1}{\sqrt{2}}\frac{-x-\sqrt{1+x^2}}{\sqrt{(1+x^2)+x\sqrt{1+x^2}}}$
8	$\frac{\sqrt{3}}{2}\frac{1}{\sqrt{2(1+x+x^2)+(1+2x)\sqrt{1+x+x^2}}}$	$\frac{1}{2}\frac{-(1+2x)-2\sqrt{1+x+x^2}}{\sqrt{2(1+x+x^2)+(1+2x)\sqrt{1+x+x^2}}}$

resonant lines, $x_{1/2} = 4\pi\tau(\nu_{1/2} - \nu)$ and $x_{3/2} = 4\pi\tau(\nu_{3/2} - \nu)$. Using eqs. (10) and β_{ij}^{+} and β_{ij}^{-} in table 3, eq. (9) can be rewritten as follows:

$$\theta_{\mathrm{P}} \simeq \frac{q_{3\mathrm{P}}c^2\nu Nl}{8\pi}\left\{\sum_i\left(\psi_{1/2}\left(P_i-\tfrac{1}{8}\right)\left(\frac{|B_iB_5'|^2}{8}-\frac{|A_iA_6'|^2}{8}\right)\right.\right.$$
$$+\psi_{3/2}\left(P_i-\tfrac{1}{8}\right)\left(\frac{|A_iA_1'|^2}{16}+\frac{|B_iB_2'|^2}{16}\right.$$
$$\left.\left.-\frac{|B_iB_4'|^2}{16}-\frac{|A_iA_3'|^2}{16}\right)\right\}$$
$$\simeq \frac{q_{3\mathrm{P}}c^2\nu Nl}{8\pi}\left(\frac{\psi_{3/2}}{24}-\frac{\psi_{1/2}}{12}\right)\sum_i\left(P_i|A_i|^2-P_i|B_i|^2\right). \tag{11}$$

On the other hand, the electronic spin polarization P can be defined as follows.

$$P=\frac{\sum_i\left(P_i|A_i|^2-P_i|B_i|^2\right)}{\sum_i\left(P_i|A_i|^2+P_i|B_i|^2\right)}=\sum_i\left(P_i|A_i|^2-P_i|B_i|^2\right). \tag{12}$$

Here $|A_i|^2+|B_i|^2=1$ and $\Sigma P_i=1$. Substituting eq. (12) into eq. (11), θ_{P} is given by the expression

$$\theta_{\mathrm{P}}=\frac{q_{3\mathrm{P}}c^2\nu Nl}{8\pi}\left(\frac{\psi_{3/2}}{24}-\frac{\psi_{1/2}}{12}\right)P. \tag{13}$$

The electronic spin polarization P can be estimated from eq. (13) by measuring the additional Faraday rotation angle θ_{P}.

Table 3
Transition probabilities between the hyperfine sublevels of the sodium ground state (3S) and excited state (3P) induced by left and right circularly polarized light.
(a) β_{ij}^{+}

i $j=$	1				2				3	4	5				6
$(F, m_F)=$	(3, 3)	(3, 2)	(3, 1)	(3, 0)	(2, 2)	(2, 1)	(2, 0)	2, −1)			(2, 2)	(2, 1)	(2, 0)	(2, −1)	
1	$\frac{\lvert A_1A_1'\rvert^2}{16}$														
2		$\frac{\lvert A_2A_1'\rvert^2}{16}$			$\frac{\lvert B_2B_2'\rvert^2}{16}$						$\frac{\lvert B_2B_5'\rvert^2}{8}$				
3			$\frac{\lvert A_3A_1'\rvert^2}{16}$			$\frac{\lvert B_3B_2'\rvert^2}{16}$						$\frac{\lvert B_3B_5'\rvert^2}{8}$			
4				$\frac{\lvert A_4A_1'\rvert^2}{16}$			$\frac{\lvert B_4B_2'\rvert^2}{16}$						$\frac{\lvert B_4B_5'\rvert^2}{8}$		
5								$\frac{\lvert B_5B_2'\rvert^2}{16}$						$\frac{\lvert B_5B_5'\rvert^2}{8}$	
6				$\frac{\lvert A_6A_1'\rvert^2}{16}$			$\frac{\lvert B_6B_2'\rvert^2}{16}$						$\frac{\lvert B_6B_5'\rvert^2}{8}$		
7			$\frac{\lvert A_7A_1'\rvert^2}{16}$			$\frac{\lvert B_7B_2'\rvert^2}{16}$						$\frac{\lvert B_7B_5'\rvert^2}{8}$			
8		$\frac{\lvert A_8A_1'\rvert^2}{16}$			$\frac{\lvert B_8B_2'\rvert^2}{16}$						$\frac{\lvert B_8B_5'\rvert^2}{8}$				

(b) β_{ij}^{-}

i	$j=$	1	2	3				4				5	6			
	$(F, m_F)=$			(2, −2)	(1, −1)	(1, 0)	(1, 1)	(0, 0)	(3, −1)	(3, −2)	(3, −3)		(2, −2)	(1, −1)	(1, 0)	(1, 1)
1							$\frlvert A_1A_3'\frrvert^2/16$									$\frlvert A_1A_6'\frrvert^2/8$
2						$\frlvert A_2A_3'\frrvert^2/16$		$\frlvert B_2B_4'\frrvert^2/16$							$\frlvert A_2A_6'\frrvert^2/8$	
3					$\frlvert A_3A_3'\frrvert^2/16$				$\frlvert B_3B_4'\frrvert^2/16$					$\frlvert A_3A_6'\frrvert^2/8$		
4				$\frlvert A_4A_3'\frrvert^2/16$						$\frlvert B_4B_4'\frrvert^2/16$			$\frlvert A_5A_6'\frrvert^2/8$			
5											$\frlvert B_5B_4'\frrvert^2/16$					
6				$\frlvert A_6A_3'\frrvert^2/16$						$\frlvert B_6B_4'\frrvert^2/16$			$\frlvert A_6A_6'\frrvert^2/8$			
7					$\frlvert A_7A_3'\frrvert^2/16$				$\frlvert B_7B_4'\frrvert^2/16$					$\frlvert A_7A_6'\frrvert^2/8$		
8						$\frlvert A_8A_3'\frrvert^2/16$		$\frlvert B_8B_4'\frrvert^2/16$							$\frlvert A_8A_6'\frrvert^2/8$	

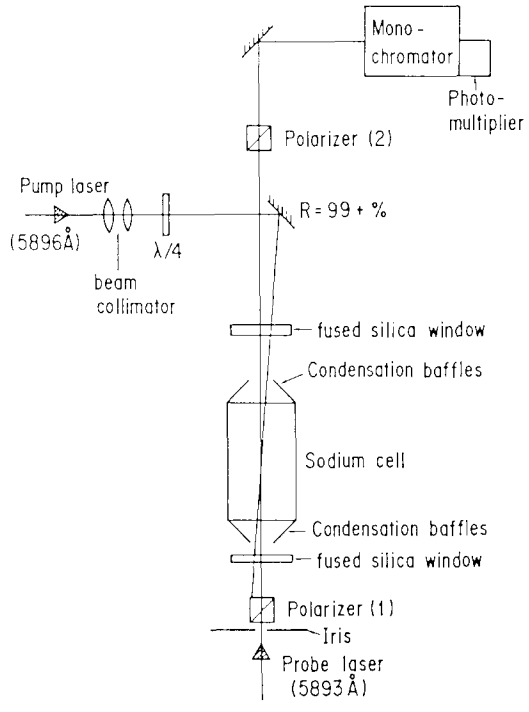

Fig. 2. Schematic of the Faraday rotation experimental apparatus.

3. Experiment

The experimental apparatus is schematically shown in fig. 2. The sodium cell was placed in a homogeneous solenoidal magnetic field of up to 4000 G. The cell was made of stainless steel and its length and diameter were 12 cm and 4 cm, respectively. The axial aperture at both ends of the cell was 4 mm.

A single frequency dye laser (Spectra Physics 380c) was used as the probe laser for the measurement of the Faraday rotation angle with attenuating its output power to about 10 mW. The wavelength of the probe laser was continuously monitored by a wavemeter (Burleigh WA-10) and tuned to an appropriate wavelength within an error of $\pm 10^{-3}$ nm. The probe beam, passing through two polarizers, was detected by a photomultiplier which was attached to a monochromator tuned to the wavelength of the probe beam. The downstream polarizer (#2) was used to detect the amount of rotation of the linearly polarized probe beam given by the sodium target located between the two polarizers. The linearly polarized laser beam, passing through the upstream polarizer (#1), underwent a Faraday rotation in the presence of sodium vapour and also a further rotation if the sodium was polarized. The angular setting of the downstream polarizer (#2), when crossed with respect to the upstream polarizer (#1) in the absence of sodium, was the reference angle θ_1. The introduction of sodium vapour produced a Faraday rotation of the probe beam and a different setting of the downstream polarizer (#2), labelled θ_2, was required in order to minimize light transmission through this polarizer. Moreover, the downstream polarizer (#2) required another different setting of the rotation angle, labelled θ_3, when the sodium vapour was polarized by optical pumping. The pumping beam was produced from another single frequency dye laser whose wavelength was tuned to the sodium D_1 line. The output power of the pumping beam was about 700 mW. A personal computer was used to make a least squares quadratic fit to eleven photomultiplier output readings, taken at 1° intervals, straddling each minimum position of θ_1, θ_2 and θ_3. The Faraday rotation angle θ_0 in eq. (8) and the additional angle θ_P in eq. (13) are obtained by the following calculations

$$\theta_0 = \theta_2 - \theta_1,$$

$$\theta_P = \theta_3 - \theta_2.$$

Each angle of θ_i $(i = 1, 2, 3)$ could be measured within an error of 0.055° and the error of θ_0 and θ_P obtained from the above equations was 0.078°.

4. Results

In order to check the theoretical calculation of Faraday rotation in a weak magnetic field, which was developed in the previous section, we have measured the rotation angle θ_0 for various strengths of the magnetic field as a function of the probe beam wavelength. During the experiment, the temperature of the sodium cell was kept constant at 230° C. The experimental results are summarized in figs. 3a–3d. Open circles in the figures show the measured θ_0 and the solid lines are the theoretically estimated θ_0 when the sodium target thickness was chosen to be $Nl = 9.95 \times 10^{13}$ n/cm^2. This target thickness was obtained from the measurement in a strong magnetic field of 1900 G.

As can be seen from the figures, the theoretically calculated rotation angles as a function of the probe beam wavelength show good agreement with the measured values for various magnetic field strengths. The systematic differences between the theoretical and experimental values could come from the effect that the actual target thickness of the sodium atoms increased very slightly during the experiment which was over a long time.

We have also measured an additional Faraday rotation θ_P induced by the polarized sodium atoms which was optically pumped by another single frequency dye laser. The measurement was done in a weak magnetic field of 200 G for various wavelengths of the probe beam. In this case, the temperature of the sodium cell

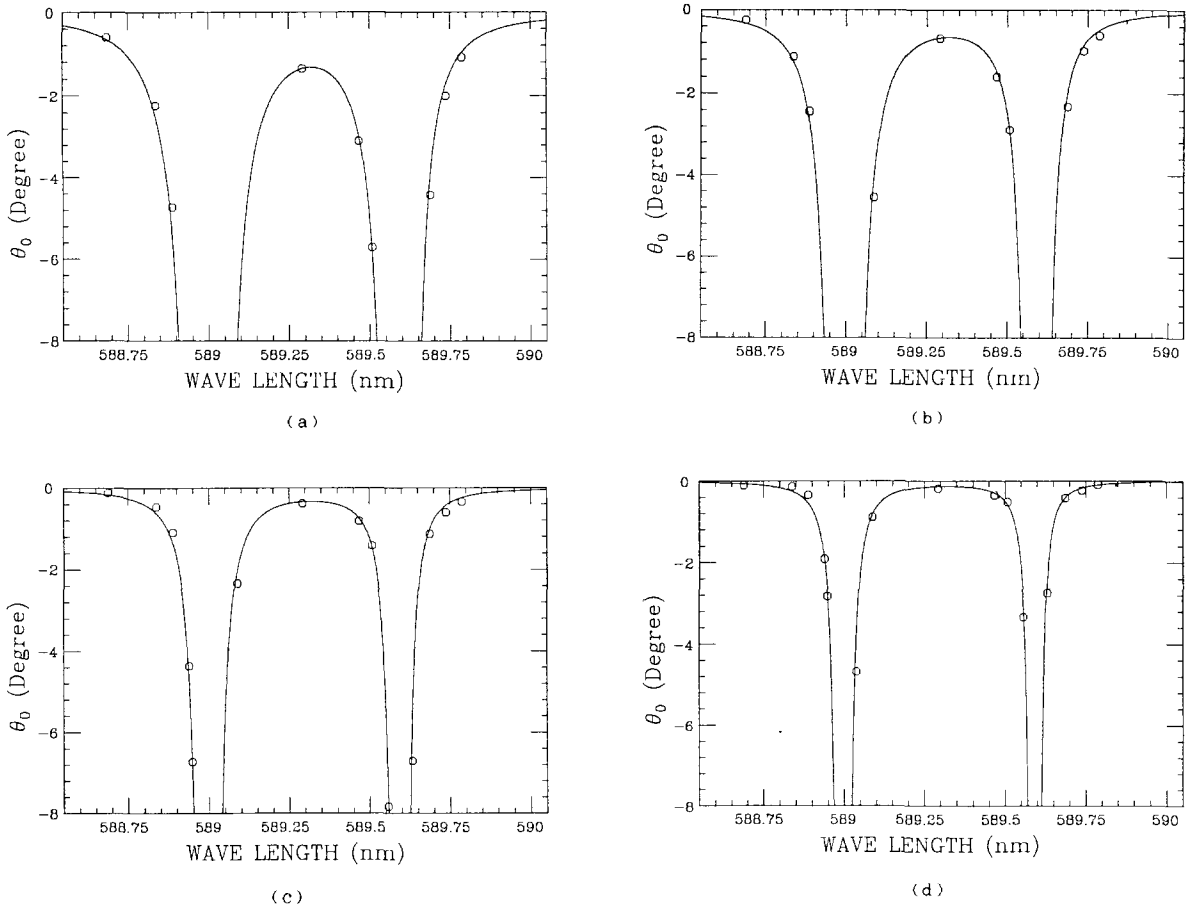

Fig. 3. Faraday rotation angle θ_0 as a function of probe laser wavelength for various magnetic field strengths for a target thickness of 9.95×10^{13} n/cm^2: (a) magnetic field strength of 1900 G; (b) 950 G; (c) 480 G; (d) 190 G. Open circles and solid lines show the measured rotation angles and theoretically calculated values, respectively.

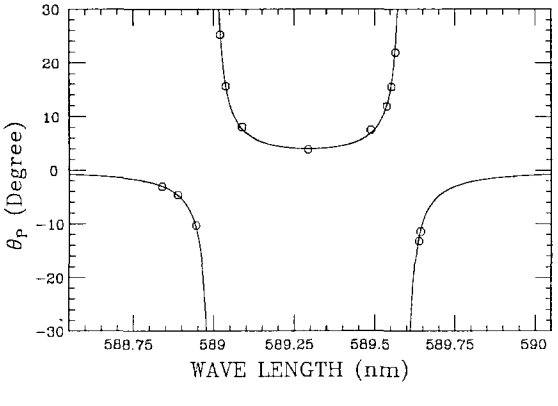

Fig. 4. Faraday rotation angle θ_P as a function of probe laser wavelength when the sodium polarization is 11%. Open circles and solid lines show the measured rotation angles and theoretically calculated values, respectively.

was kept at 220 °C. The result is shown in fig. 4. The open circles in the figure show measured values and the solid line presents the theoretical ones which are calculated from eq. (13) when the electron polarization defined in eq. (12) is taken to be 11%. This polarization seemed to be consistent with the pumping laser power of about 700 mW. The calculated values of θ_P agreed well with the measured ones even in the wide range of the wavelength of the probe beam.

5. Conclusion

The theory of Faraday rotation for sodium vapour was extended to a weak magnetic field lower than the critical field of hyperfine interaction for the calculation of target thickness and electronic spin polarization, if the vapour was optically pumped. Also, in order to

check the theory, the experiment of the Faraday rotation angles θ_0 and θ_P were performed in various weak magnetic fields for the different wavelengths of the probe beam. The agreement between the theory and the experiment was excellent and it was found that Faraday rotation was a very useful technique, even in a weak magnetic field, to examine the target thickness and the atomic polarization of optically pumped sodium. This technique could be applied to a proposed collisional pumping experiment and some other optical pumping experiments in a weak magnetic field.

Acknowledgements

The authors are indebted to Profs. Nishikawa, Kamei and Kihara for their continuous encouragement. They also appreciate Messrs. Takagi and Ikegami for their help in the experiments.

References

[1] L.W. Anderson, Nucl. Instr. and Meth. 167 (1979) 363.
[2] Y. Mori, K. Ikegami, Z. Igarashi, A. Takagi and S. Fukumoto, Proc. Workshop on Intense Polarized Proton Ion Source at Vancouver, AIP Conf. Proc. No. 117, eds., G. Roy and P. Schmor (AIP, New York, 1984) p. 123.
[3] W. Happer, Rev. Mod. Phys. 44 (1972) 170.
[4] R.M. Kulsrud, H.P. Furth and E.J. Valeo, Phys. Rev. Lett. 49 (1982) 1248.
[5] L.W. Anderson, S.N. Kaplan, R.V. Pyle, L. Ruby, A.S. Schlachter and J.W. Stearns, Phys. Rev. Lett. 52 (1984) 609.
[6] Y. Mori, K. Ikegami, A. Takagi, S. Fukumoto and W.D. Cornelius, Nucl. Instr. and Meth. 220 (1984) 264.